Displacement of SERCA from SR Lipid Caveolae-Related Domains by Bcl-2: A Possible Mechanism for SERCA Inactivation†

Elena S. Dremina, Victor S. Sharov, and Christian Schöneich*

Department of Pharmaceutical Chemistry, University of Kansas, Lawrence, Kansas 66047

Received April 29, 2005; Revised Manuscript Received October 21, 2005

ABSTRACT: Bcl-2 exerts its anti-apoptotic effect in part through the regulation of Ca^{2+} homeostasis at the level of the endoplasmic reticulum. Earlier, we demonstrated that a truncated form of Bcl-2, Bcl-2Δ21, interacts with and destabilizes the skeletal muscle sarco/endoplasmic reticulum Ca-ATPase (SERCA) [Dremina, E. S., Sharov, V. S., Kumar, K., Zaidi, A., Michaelis, E. K., and Schöneich, C. (2004) *Biochem. J. 383*, 361−370]. Here we show that (i) the transmembrane (TM) domain of Bcl-2 accelerates SERCA inactivation, (ii) both Bcl-2Δ21 and full-length Bcl-2 selectively interact with SERCA1, and (iii) the inactivation of SERCA is accompanied by a translocation of SERCA from caveolae-related domains (CRD) of the sarcoplasmic reticulum (SR). In rat skeletal muscle SR, intact SERCA1 was detected only in the CRD fractions of a sucrose density gradient. Co-incubation of SR with either Bcl-2Δ21 or full-length Bcl-2 resulted in both the appearance of Bcl-2Δ21 or Bcl-2 in the fractions containing SERCA1 and translocation of SERCA1 from CRD fractions; the latter effect correlated with the loss of the Ca-ATPase activity of the protein.

Ca^{2+} is an important mediator of many physiological processes, including the execution of apoptosis (*1*). An increase in mitochondrial Ca^{2+} levels triggers the mitochondrial permeability transition pore to release cytochrome *c* and several other pro-apoptotic proteins into the cytosol (*2*). Here cytochrome *c* becomes part of the apoptosome and induces the proteolytic activation of caspases, which regulate the execution of apoptosis (*2*−*4*). The response of mitochondria to apoptotic stimuli depends either critically or partially on the availability of Ca^{2+} from the endoplasmic reticulum (ER)[1] (*5*−*7*) through inositol 1,4,5-trisphosphate receptor (IP_3R)-mediated release (*8*, *9*). A reduction of ER Ca^{2+} levels has been associated with a protection of cells against apoptosis (*10*). Such a reduction can be achieved by the overexpression of Bcl-2 (*11*, *12*). Generally, Ca^{2+} ions are transported into the ER lumen from the cytosol by several isoforms of the sarco/endoplasmic reticulum Ca^{2+}-ATPase (SERCA). The overexpression of SERCA for genetic corrections of a low ER Ca^{2+} load restores the apoptotic response to Ca^{2+}-mobilizing stimuli (*7*). It was proposed that the regulation of ER Ca^{2+} levels serves as a general mechanism for the regulation of cellular sensitivity to various apoptotic stimuli (*7*, *10*−*13*).

The Bcl-2 protein family plays an important regulatory role for apoptosis (*14*−*17*). This family consists of both anti-apoptotic and pro-apoptotic proteins (*14*). The anti-apoptotic function of Bcl-2 may be related to its presence in the ER and mitochondrial membranes, in part, regulating apoptosis through a modulation of intracellular Ca^{2+} homeostasis (*10*−*13*). The overexpression of Bcl-2 inhibits apoptosis by preventing the redistribution of Ca^{2+} from the ER to the mitochondria (*18*, *19*), although the exact mechanisms of how Bcl-2 modulates the ER Ca^{2+} levels are still unknown. Some evidence that Bcl-2 preserves high ER Ca^{2+} concentrations through the inhibition of the IP_3R-mediated Ca^{2+} release has been provided (*20*), whereas others reported that Bcl-2 decreases ER Ca^{2+} levels by increasing the degree of leakage of Ca^{2+} from the ER (*11*, *12*). The latter findings have been supported by application of a specific sensor for imaging Ca^{2+} in the ER, directly showing that the overexpression of Bcl-2 lowers the ER Ca^{2+} load by increasing the level of Ca^{2+} leakage (*21*).

The anti-apoptotic effect of Bcl-2 may be the result of a direct interaction with important Ca^{2+}-regulating proteins in the ER. Recently, we have reported on a direct interaction of a truncated form of Bcl-2, Bcl-2Δ21, with SERCA1, which results in the inhibition of the Ca^{2+}-ATPase activity in purified rat skeletal muscle SR (*22*). This truncated form lacks the C-terminal 21-amino acid transmembrane (TM)-anchoring region. SERCA1 is the fast-twitch skeletal muscle-specific isoform of SERCA, which is highly homologous to the other isoforms, SERCA2 and SERCA3 (*23*). Co-immunoprecipitation (co-IP) experiments demonstrated formation of a complex between Bcl-2Δ21 and SERCA1 from

† This work was supported by a grant from the American Heart Association (O355555Z) and NIH Grant 2PO1AG12993.

* To whom correspondence should be addressed: University of Kansas, 2095 Constant Ave., Lawrence, KS 66047. Telephone: (785) 864-4826. Fax: (785) 864-5736. E-mail: schoneic@ku.edu.

[1] Abbreviations: CRD, caveolae-related domains; ER, endoplasmic reticulum; GM1, monosialoganglioside; GSH, glutathione; GST, glutathione *S*-transferase; HPLC, high-performance liquid chromatography; IP, immunoprecipitation; IPTG, isopropyl D-thiogalactopyranoside; IP_3R, inositol 1,4,5-trisphosphate receptor; LB, Luria−Bertani medium; NESI-MS/MS, nanoelectrospray ionization tandem mass spectrometry; PMSF, phenylmethanesulfonyl fluoride; SERCA, sarco/endoplasmic reticulum Ca-ATPase; STE, Tris-buffered saline; TM, transmembrane domain; SR, sarcoplasmic reticulum; WB, Western blot.

10.1021/bi050800s CCC: $33.50
Published on Web 12/06/2005

skeletal muscle. The inhibition of SERCA activity by Bcl-2Δ21 does not proceed through proteolytic degradation or oxidative modification of the protein in the presence of Bcl-2Δ21; however, the interaction with Bcl-2 resulted in a conformational change of SERCA1 (*22*).

In this work, we have further analyzed the mechanism of SERCA destabilization and inhibition by Bcl-2. We will demonstrate that in the SR SERCA1 is predominantly localized to specific membrane domains, which are similar in density to lipid rafts, and will be called caveolae-related domains (CRD). The presence of Bcl-2 causes a translocation of SERCA from the CRD into sucrose density fractions that are higher in density. The TM domain is not required for but accelerates the inhibition of SERCA by Bcl-2. Skeletal muscle SERCA1 was selected as an easy accessible model for the general interaction of SERCA with Bcl-2.

MATERIALS AND METHODS

Protein Expression and Purification. The clones of human Bcl-2Δ21 and full-length Bcl-2 were kindly provided by S. J. Korsmeyer (Harvard Medical School, Boston, MA). Plasmids encoding glutathione *S*-transferase (GST) fusion proteins were constructed by subcloning the respective cDNA into the pGEX3T vector (Amersham Biosciences, Piscataway, NJ). The proteins were expressed in *Escherichia coli DH1* and purified using glutathione−agarose beads and thrombin cleavage as described previously (*22*). This procedure yields ca. 150 μg of Bcl-2Δ21 or 30 μg of Bcl-2 per liter of LB medium as measured by a microassay with Coomassie Plus protein reagent (Pierce, Rockford, IL). Purified proteins were characterized by SDS−PAGE and Western blot (WB) analysis.

Isolation of Sarcoplasmic Reticulum. Native SR vesicles (light fraction) were prepared from 5−6-month-old Fisher 344 rat hind limb skeletal muscle (fast-twitch fibers) as described previously (*24*). Briefly, muscles (usually 20−30 g) were homogenized in a Waring blender for 1 min at maximal speed at 4 °C in 3 volumes of buffer containing 0.1 M KCl, 0.1 mM EDTA, and 20 mM MOPS (pH 7.4). The homogenate was centrifuged at 5000*g* for 20 min to remove cell debris; the pellet was washed again under the same conditions, and the pooled supernatants were centrifuged at 11800*g* for 20 min to pellet the mitochondria. To dissolve myosin, the supernatant was filtered through six layers of cheesecloth and solid KCl was added to make a final concentration of 0.6 M. After incubation for 20 min, the SR was pelleted at 23500*g* for 1 h. The supernatant was decanted, and the pellets were resuspended in a medium containing 0.3 M sucrose and 20 mM MOPS (pH 7.0) and centrifuged for 30 min at 100000*g*. SR vesicles were resuspended in a small volume of medium consisting of 0.3 M sucrose and 20 mM MOPS (pH 7.0) using a dounce homogenizer, aliquoted, quickly frozen in liquid nitrogen, and stored at −70 °C. Protein concentrations were measured with a microassay with Coomassie Plus protein reagent (Pierce). The fraction of SERCA1 in the SR determined by densitometry of Coomassie Blue-stained gels was ca. 40% relative to total protein.

Incubations of SERCA and SERCA Activity Assays. For incubations, the concentrated SR suspension (≥20 mg of SR protein/mL) was diluted to achieve a final concentration of 0.4−1 mg of SR protein/mL in STE buffer with a minimal contribution of the SR storage buffer to the incubation medium (<5%). SR was incubated with recombinant Bcl-2 or Bcl-2Δ21 (0−0.5 mg/mL) in STE buffer in plastic tubes without agitation at 37 °C in a dry thermostat. PMSF (1 mM) was added to prevent proteolytic degradation of the proteins if not stated otherwise.

Total, Ca^{2+}-dependent, and basal ATPase activities of SERCA in the SR were determined at 25 °C by a colorimetric assay of inorganic phosphate (P_i) in the presence or absence of the calcium ionophore, A23187 (*25*), as outlined in our previous paper (*22*). In all our experiments, the measured Ca^{2+}-dependent ATP hydrolysis was attributed to SERCA because the Ca^{2+}-dependent Ca-ATPase activity was completely inhibited by the addition of 20 μM thapsigargin (Sigma, St. Louis, MO).

Preparation of CRD. For the isolation of caveolae-related domains (CRD), SR was lysed in 2 mL of ice-cold 0.5 M sodium carbonate buffer (pH 11) using 20 strokes of a Dounce glass homogenizer followed by sonication. The homogenate was adjusted to 45% (w/v) sucrose by the addition of 90% sucrose in MBS buffer containing 25 mM MES (pH 6.5), 150 mM NaCl, 5 mM EDTA, and 1 mM PMSF and placed in the bottom of an ultracentrifuge tube. A discontinuous sucrose gradient was established by overlaying this solution with 4 mL of 38% sucrose and 3 mL of 5% sucrose (both sucrose solutions prepared in MBS containing 0.25 M sodium carbonate). The tube was then centrifuged at 4 °C for 16−18 h at 130000*g* in an SW41 rotor using an L90K ultracentrifuge (Beckman Coulter, Inc., Fullerton, CA). The first 2 mL fraction from the top of the gradient was discarded, and for some experiments, eight fractions (two to four 0.5 mL fractions for the CRD flotation region, and 1.5 mL fractions for the rest of the gradient) or four fractions (one and two 1.5 mL fractions and three and four 3 mL fractions) were manually collected from the top of the gradient. To determine the distribution of CRD-associated proteins within the gradient, each fraction was analyzed by SDS−PAGE, followed by WB analysis with appropriate antibodies.

SDS−PAGE and WB Analyses. The samples were separated on precast Bio-Rad 4 to 20% gradient gels using tris-glycine running and sample buffers (Invitrogen, Carlsbad, CA). The gels were then either stained for proteins by Coomassie Blue or electroblotted onto a 0.45 μm polyvinyl difluoride (PVDF) membrane (Millipore, Billerica, MA) prior to Western blot analysis. The spots were visualized by the ECL or ECL-Plus detection kit (Amersham Biosciences) according to the manufacturer's procedure.

Antibodies. Mouse monoclonal anti-Bcl-2 (sc-7382) and rabbit polyclonal anti-Bcl-2 antibodies (sc-783) were purchased from Santa Cruz Biotechnology (Santa Cruz, CA), mouse monoclonal anti-caveolin-1 antibodies (catalog no. 610059) from BD Biosciences (San Jose, CA), and rabbit polyclonal anti-caveolin-3 antibodies (catalog no. 61420) from BD Transduction Lab (San Diego, CA). Anti-SERCA1 (MA3-912) rabbit polyclonal and mouse anti-SERCA2 (MA3-910) antibodies were from Affinity Bioreagents (Golden, CO). Secondary horseradish peroxidase (HRP)-conjugated anti-rabbit antibodies were from Sigma, and HRP-conjugated anti-mouse antibodies were from Pierce Biotechnology.

Solution Binding Assay. To monitor the association between SERCA1 and Bcl-2, 100 μg of SR in lysis buffer containing 10 mM Tris-HCl (pH 7.4), 10 mM EDTA, 1% Nonindet P-40, 1 mM PMSF, and protease inhibitors (Roche Diagnostics, Indianapolis, IN) was incubated with 5 μg of GST−Bcl-2 or GST alone for 2 h at 4 °C. Following the incubation with 10 μL (packed volume) of glutathione (GSH)−Sepharose beads for 2 h, the beads were separated by centrifugation at 10 000 rpm and washed six times with the lysis buffer. To monitor the interactions between SERCA1 and Bcl-2Δ21, 500 μg of SR protein was solubilized in the buffer described above and 50 μg of GST−Bcl-2Δ21 was added, following the incubation with 30 μL (packed volume) of GSH−Sepharose beads. Proteins were separated by SDS−PAGE.

Nanoelectrospray Ionization Tandem Mass Spectrometry of In-Gel Tryptic Digests. Protein bands of interest were excised from the gel and processed as described elsewhere (*26*, *27*). In-gel tryptic digests (2 μL) were submitted to nanoelectrospray ionization tandem mass spectrometry (NSI-MS/MS) analysis on a ThermoElectron (San Jose, CA) LCQ Duo instrument equipped with a nanospray source (ThermoElectron). Separation of tryptic peptides was achieved online prior to MS/MS analysis on a BioBasic C18 nanoflow column (300 Å, 10 cm × 75 μm, 15 μm tip size) (New Objective, Woburn, MA) as outlined in our previous work (*26*). Protein sequence analysis was achieved with the ThermoElectron Bioworks 3.1 software package and the NCBI protein database downloaded from ftp.ncbi.nlm.nih.gov/blast/db.

Immunofluorescence Analysis. Normal human NPCI$^{+/+}$ (CRL-2076) fibroblasts were kindly provided by J. Krise (Department of Pharmaceutical Chemistry, University of Kansas). The cells were grown on poly-D-lysine-coated coverslips in RPMI 1640 medium supplemented with 10% fetal calf serum, 10 mM Hepes, 1 mM sodium pyruvate, and 1% penicillin/streptomycin (Invitrogen Corp.). Coverslips were gently washed three times with ice-cold PBS, and fixed with 300 μL of PBS containing 2% (w/v) paraformaldehyde, 3% sucrose, and 0.02% sodium azide, for 10 min at 25 °C. After being blocked with 5% (w/v) BSA in PBS for 10 min, the cells were permeabilized with 0.2% (v/v) Triton X-100 in PBS for 5 min at 25 °C. The coverslips were washed three times in PBS, and then incubated with appropriate primary antibodies (1:500 dilution in blocking solution) for 90 min at 25 °C. After being washed, the coverslips were incubated with AlexaFluor 488 (green) goat anti-rabbit (1:500 dilution in blocking solution) or AlexaFluor 594 (red) goat anti-mouse (1:500 dilution in blocking solution) (Molecular Probes, Eugene, OR) secondary antibodies for 30 min at 25 °C in the dark. After the solution had been washed six times in PBS, anti-fade solution (Molecular Probes) was added, and the coverslips were mounted on glass slides. Images were captured on an LSM 510 META confocal microscope (Carl Zeiss AG, Göttingen, Germany). Cells with typical morphology are presented.

RESULTS

Expression and Purification of Bcl-2. To analyze the role of the transmembrane hydrophobic domain (TM) of Bcl-2 with regard to its ability to inactivate SERCA1, the cDNAs

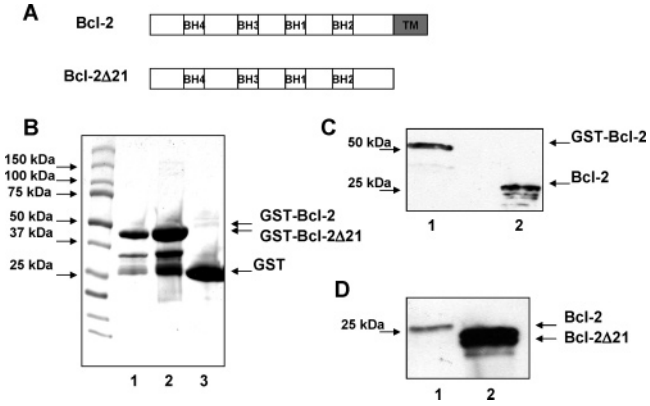

FIGURE 1: Expression and purification of full-length Bcl-2. (A) Schematic representation of the domain structures of Bcl-2 and Bcl-2Δ21. (B) SDS−PAGE of the proteins from bacterial lysate bound to glutathione−agarose beads: lane 1, 20 μg of total affinity-purified protein, i.e., GST and GST−Bcl-2Δ21; lane 2, 100 μg of GST or GST−Bcl-2Δ21; and lane 3, 100 μg of GST or GST−Bcl-2. (C) Western blot detection of GST−Bcl-2 after incubation of glutathione−agarose beads with bacterial lysate (lane 1) and Bcl-2 after thrombin cleavage (lane 2) for 4 h. (D) Western blot detection of 0.2 μg of purified Bcl-2 (lane 1) and Bcl-2Δ21 (lane 2) after thrombin cleavage of the respective GST fusion proteins.

of full-length Bcl-2 and Bcl-2Δ21 were cloned into expression vectors and proteins were expressed in *E. coli*. Schematic representations of the two proteins displaying the location of important domains are given in Figure 1A. The yield of affinity-purified full-length Bcl-2 was significantly lower than that of Bcl-2Δ21, as expected for a protein with the additional membrane-anchoring hydrophobic region. Figure 1B shows the difference in expression yields of GST−Bcl-2Δ21 and GST−Bcl-2 after induction of protein expression with IPTG. Coomassie staining of SDS−PAGE analysis shows that affinity purification with glutathione−agarose beads results in good yields of GST−Bcl-2Δ21 (Figure 1B, lanes 1 and 2). On the other hand, significantly lower yields of GST−Bcl-2 were obtained, contaminated with a large amount of copurifying GST (Figure 1B, lane 3). WB analysis of GST−Bcl-2 with an anti-Bcl-2 antibody showed a band with an apparent molecular mass of 50 kDa that corresponds to the theoretical size of GST−Bcl-2 (Figure 1C); the incubation with thrombin yields a protein with an apparent molecular mass of ca. 26 kDa (Figure 1C). Figure 1D displays the results of WB analysis for purified Bcl-2 and Bcl-2Δ21 with an anti-Bcl-2 antibody, showing a difference in the molecular size and immunoaffinity of both Bcl-2 sequences for the selected antibodies. It appears that Bcl-2Δ21 shows a significantly higher affinity for the anti-Bcl-2 antibody. Note that for Bcl-2Δ21, two closely migrating bands can be resolved. We assume that Bcl-2Δ21 may undergo some hydrolytic and/or proteolytic cleavage during processing, which is responsible for the lower of the two bands.

Effect of Bcl-2Δ21 and Bcl-2 on SERCA1 Activity. SR was incubated with different amounts of Bcl-2Δ21 in the presence or absence of 1 mM PMSF at 37 °C. Figure 2A shows plots of Ca^{2+}-ATPase activity versus incubation time in the presence of Bcl-2Δ21. At a Bcl-2Δ21:SERCA1 molar ratio of 1:1, the Ca^{2+}-ATPase activity was strongly inhibited within 2 h, whereas SR in the absence of Bcl-2Δ21 did not significantly change the activity even after incubation for 4

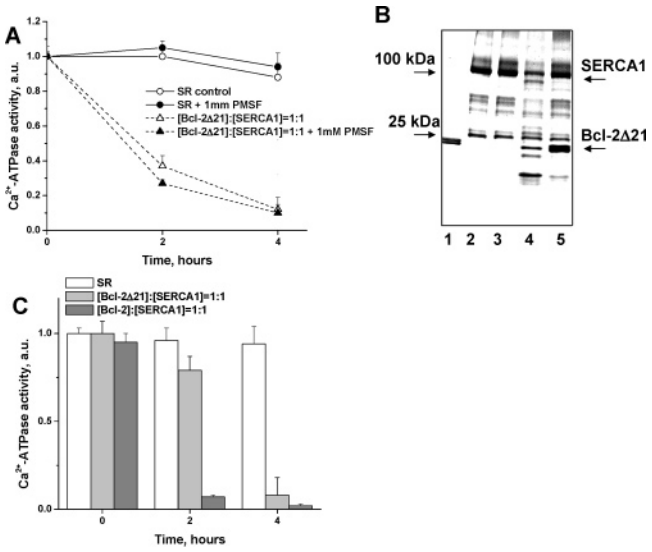

FIGURE 2: Effect of Bcl-2 and Bcl-2Δ21 on the Ca^{2+}-ATPase activity of SERCA1. (A) Time-dependent inactivation of Ca^{2+}-ATPase activity of SERCA1. SR (1 mg/mL protein) was incubated in STE buffer at 37 °C without (empty symbols) or with 1 mM PMSF (filled symbols) in the presence of Bcl-2Δ21: (○) without Bcl-2Δ21 and (△) at a 1:1 Bcl-2Δ21:SERCA1 ratio. (B) Protection of SERCA1 against degradation and enhancement of the Bcl-2Δ21 effect by PMSF. Proteins after incubation of SR with Bcl-2Δ21 for 4 h at 37 °C were separated by SDS−PAGE and stained with Coomassie Blue: lane 1, Bcl-2Δ21 (7 μg) in the presence of 1 mM PMSF; lane 2, SR without PMSF; lane 3, SR with 1 mM PMSF; and lanes 4 and 5, SR after incubation with Bcl-2Δ21 at a 1:1 Bcl-2Δ21:SERCA1 molar ratio without PMSF and with 1 mM PMSF, respectively. (C) Comparison of Bcl-2Δ21 and full-length Bcl-2 with respect to SERCA inhibition. SR (0.4 mg/mL protein) was incubated in STE buffer at 37 °C with 1 mM PMSF without and with Bcl-2Δ21 or Bcl-2 at a molar ratio to SERCA1 of 1:1, and aliquots were analyzed for Ca^{2+}-ATPase activity after incubation for 0, 2, and 4 h.

h either with or without the addition of protease inhibitors. Importantly, the inactivation of SERCA1 was not due to any proteolytic degradation of the proteins. For example, the presence of 1 mM PMSF (Figure 2B, lanes 3 and 5) or Roche protease inhibitors (data not shown) enhanced the inhibitory effect of Bcl-2Δ21 (Figure 2A).

Full-length Bcl-2 and Bcl-2Δ21 were compared with regard to their ability to destabilize and inhibit the SR Ca^{2+}-ATPase activity. Both proteins inhibited SERCA activity in a concentration- and time-dependent manner. Full-length Bcl-2 and Bcl-2Δ21 had similar effects on SERCA1 activity after incubation for 4 h (Figure 2C), demonstrating that the TM domain is not required for SERCA inactivation. However, after incubation for 2 h at a molar ratio of 1:1 (Figure 2C), full-length Bcl-2 inhibited SERCA1 to a higher extent, suggesting that full-length Bcl-2 associates more efficiently with SERCA1 and/or is incorporated more rapidly into the SR membranes.

Association of Bcl-2 and SERCA1. Previously, we demonstrated that low levels of endogenous Bcl-2 can be detected in the SR, and that Bcl-2Δ21 forms a complex with SERCA1 (*22*). To demonstrate a direct interaction of SERCA1 with full-length Bcl-2, we employed a binding assay based on copurification of SERCA1 with added GST−Bcl-2. GST−Bcl-2 or, for control, GST alone was incubated with SR for 2 h, and affinity-purified proteins were analyzed by WB analysis. Figure 3A shows a WB analysis of GST−Bcl-2

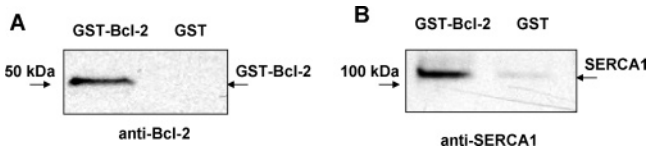

FIGURE 3: Association of Bcl-2 with SERCA1. SR (100 μg of protein) was incubated with 5 μg of GST−Bcl-2 or 5 μg of GST alone (A and B) prior to the addition of protein A−agarose beads for isolation of copurified SERCA1 as described in Materials and Methods, followed by WB analysis with anti-Bcl-2 (A) or anti-SERCA1 (B) antibodies.

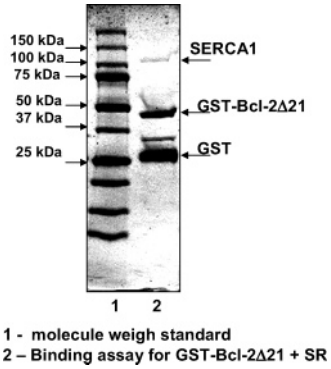

FIGURE 4: SERCA1 is the main protein of SR interacting with Bcl-2Δ21. GST−Bcl-2Δ21 (50 μg) was incubated with 500 μg of protein SR (lane 2) prior to the addition of protein A−agarose beads for isolation of copurified proteins followed by a separation by SDS−PAGE and Coomassie blue staining.

and GST with the anti-Bcl-2 antibody, confirming the presence of Bcl-2 only in the fusion protein. Figure 3B displays the results of WB analysis with an anti-SERCA1 antibody, showing that SERCA1 specifically associates with GST−Bcl-2 but not with GST alone.

SERCA1 Is the Main Protein Target for Bcl-2Δ21 in the SR. To determine all potential SR protein targets for Bcl-2 and to estimate the stoichiometry of the Bcl-2−SERCA1 complex, we affinity-purified SR proteins with GST−Bcl-2Δ21. GST−Bcl-2Δ21 at a final GST−Bcl-2Δ21:SERCA1 molar ratio of 1:1 was added to our SR preparations. After incubation for 2 h, the affinity-purified SR proteins bound to GST−Bcl-2Δ21 were separated by SDS−PAGE and visualized with Coomassie Blue staining (Figure 4). In a control experiment, GST−Bcl-2Δ21 alone was subjected to SDS−PAGE separation and Coomassie Blue staining. SDS−PAGE revealed that the affinity-purified SR proteins yielded an additional single band at ca. 110 kDa. This band was digested in gel with trypsin, and the digest was analyzed by NSI-MS/MS, identifying six peptides of the rat SERCA1 sequence covering ca. 15% of the total protein sequence (Y^{36}-GPNELPAEEGK^{47}, D^{237}QMAATEQDKTPLQQK^{252}, V^{437}-GEATETALTTLVEK^{451}, I^{638}GIFSENEEVADR^{651}, E^{656}-FDDLPLAEQR^{667}, and I^{686}VEYLQSYDEITAMTGDGVND-APALK^{722}). Thus, SERCA1 appears to be the major protein interacting with Bcl-2Δ21 in our SR preparation. Importantly, the intensity of the SERCA1 band is significantly lower compared to that of GST−Bcl-2Δ21 used in the assay. Therefore, under our experimental conditions, the binding of Bcl-2Δ21 to SERCA1 appears not to be stoichiometric. Physiologically, this result is absolutely reasonable (see the Discussion).

Distribution of Caveolin-1 and Caveolin-3 in CRD of the SR. Our earlier results indicated a partial unfolding of

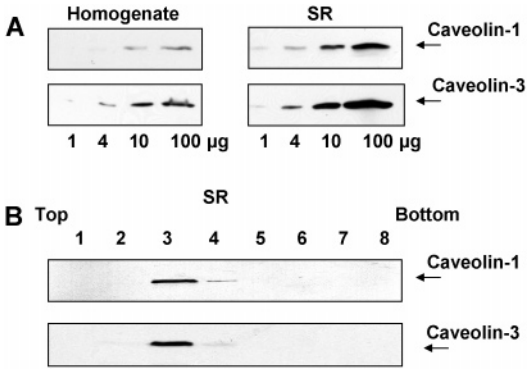

FIGURE 5: Expression of caveolin-1 and caveolin-3 in skeletal muscle tissue. (A) Tissue homogenate and SR were subjected to WB analysis using anti-caveolin-1 and anti-caveolin-3 antibodies. Protein amounts are given for the respective lanes. (B) SR was fractionated by sucrose density gradient centrifugation. Fractions were collected and analyzed by WB with anti-caveolin-1 and anti-caveolin-3 antibodies. Fraction numbers are given for the respective lanes.

SERCA1 upon incubation of SR with Bcl-2Δ21 which may be related to the loss of SERCA1 activity (*22*). Here, we will present evidence that association with Bcl-2 can actually induce a translocation of SERCA1 from specific membrane domains, CRD, into a different membrane environment. We detected caveolin-1 and caveolin-3 in the skeletal muscle homogenate and in the purified SR (Figure 5A). Usually, caveolin represents a protein marker of caveolae-related domains (CRD) in the plasma membrane (*28*). However, the presence of caveolins in the ER membrane has been documented, and is necessary for cholesterol transport (*45*). To study the formation of CRD in the SR membrane, we fractionated SR by sucrose density gradient centrifugation to separate fractions of membrane microdomains with different buoyant densities. The results presented in Figure 5B indicate that caveolin-1 and caveolin-3 target to the 5%−35% interface of the sucrose density gradient, a low-buoyant density CRD fraction (Figure 5B, fractions 3 and 4). Our results indicate that SR purified from skeletal muscle contains CRD-like domains that can be characterized by colocalization with caveolin-1 and caveolin-3 through sucrose density gradient fractionation of SR.

Effect of Bcl-2 on the Distribution of SERCA1 during Sucrose Density Gradient Fractionation. We fractionated SR in the absence and presence of various amounts of added Bcl-2Δ21, by sucrose density gradient centrifugation. We used Bcl-2Δ21 due to the high expression yields. In the absence of Bcl-2Δ21, WB analysis of SR proteins detected SERCA1 in three 0.5 mL low-buoyant density fractions (lanes 2−4 in Figure 6A) close to the 5%−35% interface of the sucrose density gradient. In control experiments, Bcl-2Δ21 alone was detected mostly on the bottom of the gradient (Figure 6B, fractions 6−8), i.e., fractions with a maximal density. The coexistence of SERCA1 with caveolin-1 and caveolin-3 in the same fractions (see Figure 5B) suggests that SERCA1 is located in CRD-like domains of skeletal muscle SR (see the Discussion). These features change when Bcl-2Δ21 is added to the SR. After co-incubation for 2 h with the SR at 37 °C, Bcl-2Δ21 partially associated with the CRD and colocalized with SERCA1 (Figure 6D,F). In addition, a shift in the SERCA1 distribution to fractions 3−5 (Figure 6C) and 6−8 (Figure 6E) is observed, depending on the Bcl-2Δ21:SERCA1 molar ratios, 1:4 and 2:1, respectively. At the molar ratio of 2:1, which caused a pronounced displacement of SERCA1 from frac-

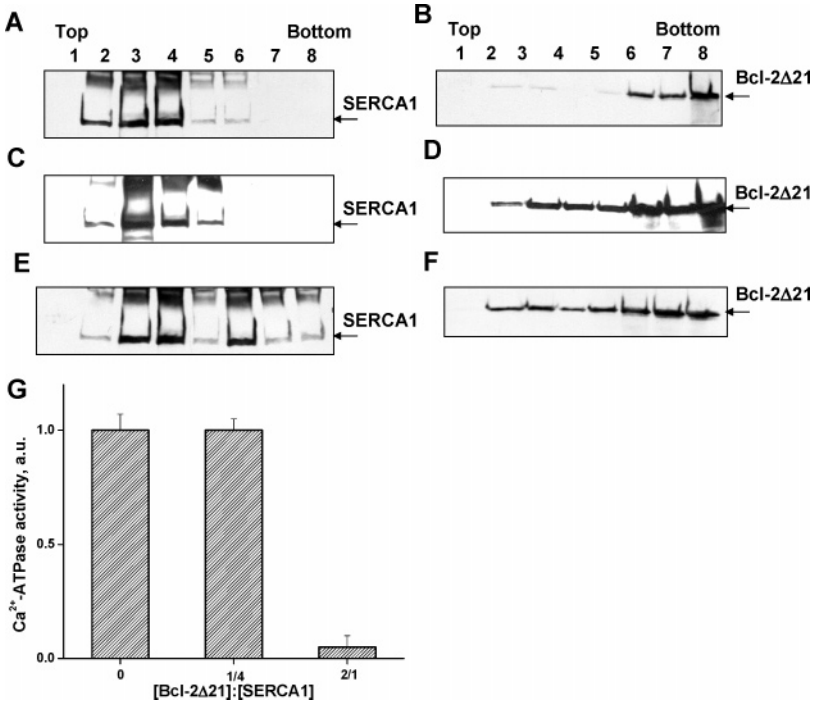

FIGURE 6: Sucrose gradient fractionation of SR and the effect of Bcl-2Δ21. SR and Bcl-2Δ21 at different molar ratios were incubated in STE buffer at 37 °C in the presence of 1 mM PMSF for 2 h followed by sucrose density gradient separation. Fractions were collected and analyzed by WB with anti-SERCA1 (in panels A, C, and E) anti-Bcl-2 (in panels B, D, and F) antibodies. Fraction numbers are given for the respective lanes. Separation has been performed for the SR alone (A), Bcl-2Δ21 alone (B), and at a 1:4 (C and D) or 2:1 Bcl-2Δ21:SERCA1 molar ratio (E and F). (G) Ca^{2+}-ATPase activity in the SR samples after incubation with Bcl-2Δ21 measured prior to sucrose density gradient fractionation.

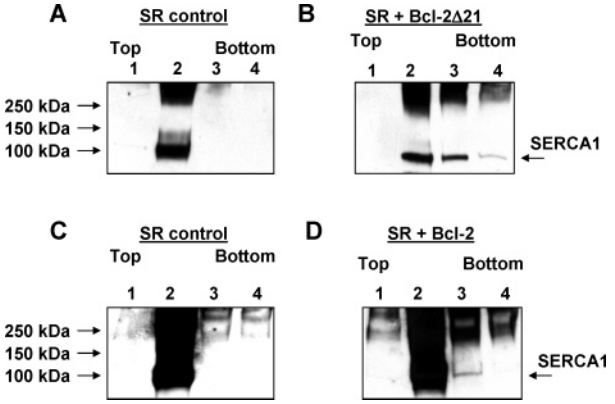

FIGURE 7: Sucrose gradient fractionation of SR. Comparison of Bcl-2 and Bcl-2Δ21. SR without addition (A and C) or in the presence of Bcl-2Δ21 (B) or Bcl-2 (D) at a 2:1 Bcl-2: or Bcl-2Δ21:SERCA molar ratio was incubated in STE buffer at 37 °C in the presence of 1 mM PMSF for 4 h, followed by sucrose density gradient separation. Fractions were collected and analyzed by WB with anti-SERCA1 antibodies. Fraction numbers are given for the respective lanes. In panels A and B, 250 μg of SR was subjected to sucrose density gradient separation and 0.005 mL of each fraction was analyzed with a WB. In panels C and D, 25 μg of SR was subjected to sucrose density gradient separation and 0.05 mL of each fraction was analyzed with a WB.

tions 2−4 to fractions 6−8, at the bottom of the gradient (Figure 6E), a virtually complete loss of Ca^{2+}-ATPase activity was observed (Figure 6G). It is important to note that, although Bcl-2Δ21 colocalized with SERCA1 in low-buoyant density fractions, a relatively large amount of Bcl-2Δ21 remained in the high-density fractions on the bottom of the gradient (Figure 6D,F), consistent with a substoichiometric binding of Bcl-2Δ21 to SERCA1 (see above).

We then compared full-length Bcl-2 and Bcl-2Δ21 with regard to their ability to induce a translocation of SERCA1 from CRD of SR. For this experiment, SR was incubated at a molar ratio of 2:1 for Bcl-2:SERCA1 or Bcl-2Δ21:SERCA1 for 4 h at 37 °C, and a complete inhibition of SERCA1 activity was detected for both Bcl-2 and Bcl-2Δ21 (data not shown). Because of the low expression yields of Bcl-2, the experiment for Bcl-2 was performed with a 10 times smaller amount of both Bcl-2 and SR to adjust the required Bcl-2:SERCA1 molar ratio of 2:1. Hence, for a satisfactory detection of the SERCA1 distribution in the sucrose density fractions, 10 times larger amounts of each fraction were loaded onto the gel for Western blot analysis (Figure 7). Four fractions were collected from the top of the gradient, where fraction 2 represents the CRD fraction, indicated by Western blot analysis. Because of the high sucrose content loaded onto the gel in the case of the Bcl-2 experiments, the SERCA1 band in CRD fraction 2 appears more smeared (cf. panels A and C of Figure 7). Both Bcl-2 and Bcl-2Δ21 promote translocation of SERCA1 from CRD after incubation for 4 h at a molar ratio of 2:1 (Figure 7B,D). However, during the incubation with full-length Bcl-2, a higher level of SERCA1 dimers was detected on the bottom fractions of the sucrose gradient, compared to that for higher-molecular weight oligomers for incubation with Bcl-2Δ21. The reason for this difference is not clear. SERCA aggregation may be caused by translocation through Bcl-2/Bcl-2Δ21 as well as the sucrose density gradient centrifugation itself. The higher sucrose content of the full-length Bcl-2-containing fractions may prevent the transition from dimer to oligomer.

Effect of Bcl-2 on Caveolin-1 and Caveolin-3 Distribution during Sucrose Density Gradient Fractionation. We have shown above that caveolin-1 and caveolin-3 colocalize with SERCA1 in CRD fractions of SR sucrose density gradient centrifugation (Figure 5B, fractions 3 and 4). To study the effect of Bcl-2 on localization of caveolin-1 and caveolin-3 in the CRD fractions, we fractionated SR by sucrose density gradient centrifugation after incubation for 4 h at 37 °C in the presence of Bcl-2Δ21 or Bcl-2 at a Bcl-2:SERCA1 or Bcl-2Δ21:SERCA1 molar ratio of 2:1, i.e., conditions under which complete inhibition of SERCA activity was detected (data not shown). Figure 8 shows the Western blot analysis of the caveolin-1 and caveolin-3 distribution prior to and after incubation of SR with Bcl-2Δ21 or Bcl-2. The experiment with full-length Bcl-2 was performed with 10 times smaller absolute amounts of protein and SR. Four

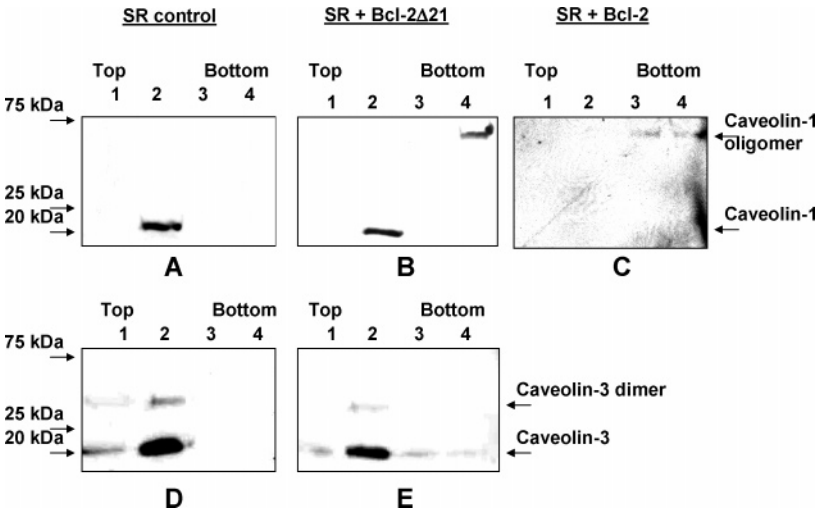

FIGURE 8: Redistribution of caveolin-1 and caveolin-3 by Bcl-2 and Bcl-2Δ21. SR in the absence (A and D) or in the presence of Bcl-2Δ21 (B and E) or Bcl-2 (C) at a 2:1 Bcl-2: or Bcl-2Δ21:SERCA molar ratio was incubated in STE buffer at 37 °C in the presence of 1 mM PMSF for 4 h, followed by sucrose density gradient separation. Fractions were collected and analyzed by WB with anti-caveolin-1 (A−C) and anti-caveolin-3 (D and E) antibodies. Fraction numbers are given for the respective lanes. In panels A, B, D, and E, 250 μg of SR was subjected to sucrose density gradient separation and 0.005 mL of each fraction was analyzed with a WB. In panel C, 25 μg of SR was subjected to sucrose density gradient separation and 0.05 mL of each fraction was analyzed with a WB.

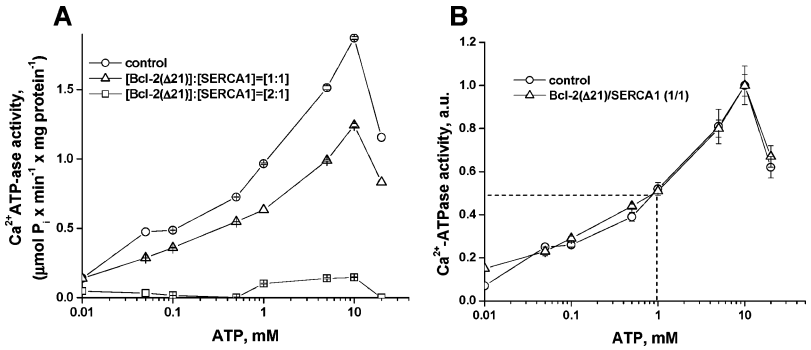

FIGURE 9: Effect of Bcl-2Δ21 on the ATP-dependent activation of SERCA1. (A) SR (1 mg/mL protein) was incubated for 2 h at 37 °C in STE buffer containing 1 mM PMSF without Bcl-2Δ21 (○) and at a Bcl-2Δ21:SERCA1 molar ratio of 1:1 (△) or 2:1 (□) prior to the analysis of Ca^{2+}-ATPase activity in the presence of different ATP concentrations. (B) Concentration dependences normalized to the maximal activities for the respective curves. Dashed lines illustrate the determination of the half-maximal ATP concentration ($K_{0.5}$).

fractions were collected from the top of the gradient, where fraction 2 represents the CRD fraction. After co-incubation of SR with Bcl-2Δ21 for 4 h, a partial decrease in the caveolin-1 level (Figure 8A,B, lane 2) and a similar decrease in the caveolin-3 level (Figure 8D,E, lane 2) in the CRD fraction were observed. This is accompanied by the detection of a caveolin-1 oligomer (Figure 8B, lane 4) and caveolin-3 monomers (Figure 8E, lanes 3 and 4) in the bottom fractions of the gradient. A similar analysis of caveolin-1 after co-incubation of SR for 4 h with full-length Bcl-2 showed a rather complete absence of caveolin-1 in the CRD fraction (Figure 8C), accompanied by the detection of caveolin-1 oligomer in the bottom fractions of the gradient.

Effect of Bcl-2Δ21 on the Apparent ATP Affinity of SERCA1. We had shown that the inhibition of SERCA1 by Bcl-2Δ21 is not due to a change in the Ca^{2+} affinity of the high-affinity Ca^{2+}-binding domain of SERCA1 (*22*). Here, we have characterized the effect of Bcl-2Δ21 on the ATP affinity of SERCA1. The incubation of SR with Bcl-2Δ21 for 2 h inhibited the SERCA1 activity by ca. 30% for a 1:1 Bcl-2Δ21:SERCA1 molar ratio, and nearly completely for a 2:1 molar ratio independent of the ATP concentration (Figure 9A). Importantly, for an equimolar Bcl-2Δ21:SERCA1 ratio, the lost activity of SERCA1 can be restored to control values by increasing the concentration of ATP by ca. 10-fold for all ranges of applied ATP concentrations. However, analysis of the normalized curves (Figure 9B) shows that the ATP concentration for half-maximal activation ($K_{0.5} \sim 1 \times 10^{-6}$ M under our conditions) did not change in the presence of Bcl-2Δ21, suggesting that the inhibition of SERCA1 activity by Bcl-2Δ21 is not related to either competition for the ATP-binding domain of SERCA1 or allosteric regulation of the ATP-binding domain.

Partial Colocalization of Endogenous SERCA2 with Bcl-2 and Caveolin-1 in NPCI$^{+/+}$ Cells by Double-Staining Immunofluorescent Confocal Microscopy. We examined the subcellular colocalization of SERCA2, Bcl-2, and caveolin-1 by double-staining immunofluorescent confocal microscopy. For this, we used normal NPCI$^{+/+}$ human fibroblast cells, which express all proteins of interest at a sufficiently high level required for immunofluorescent microscopy analyses. This change to NPCI$^{+/+}$ fibroblasts was necessitated by the fact that the natural Bcl-2 abundance in skeletal muscle SR is too low for immunofluorescence microscopy [detection of Bcl-2 in purified skeletal muscle SR required immunoprecipitation (*22*)]. However, these experiments will show

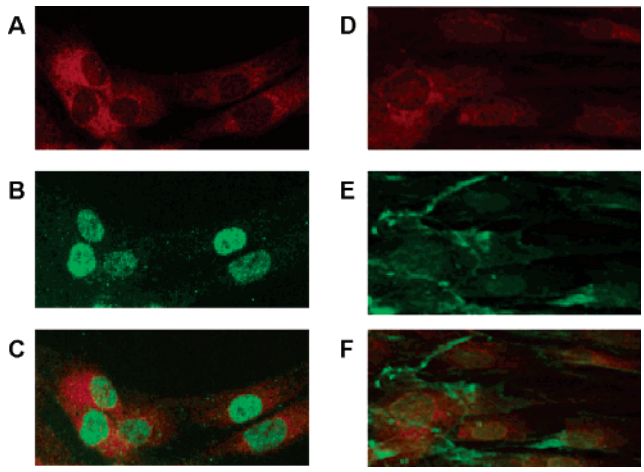

FIGURE 10: Partial colocalization of endogenous SERCA2 with Bcl-2 or caveolin-1 in NPCI$^{+/+}$ cells by double-staining immunofluorescent confocal microscopy. Cells were stained for SERCA2 (A) and Bcl-2 (B). Merged images show the partial colocalization (yellow) of Bcl-2 with SERCA2 (C). Cells were stained for SERCA2 (D) and caveolin-1 (E). Merged images show the partial colocalization (yellow) of caveolin-1 with SERCA2 (F).

that the SERCA−Bcl-2 interaction is not limited to skeletal muscle SR. Cells were doubly labeled with a monoclonal antibody for SERCA2 and a polyclonal antibody against Bcl-2 or caveolin-1. Endogenously expressed SERCA2 displays a dominant localization in the cytoplasm at the perinuclear region, consistent with ER localization (Figure 10A,D). Endogenously expressed Bcl-2 is localized predominantly to the nucleus, and weak staining is detected in the cytoplasm with patterns consistent with mitochondrial localization (Figure 10B). Image overlay shows a partial colocalization of these two proteins in the cytoplasm at the perinuclear region of the ER (Figure 10C). Endogenously expressed caveolin-1 is localized to the plasma membrane and the cytoplasm (Figure 10E), and image overlay shows the partial colocalization of SERCA2 and caveolin-1 in the perinuclear region representing the ER (Figure 10F). Thus, the data from double-staining immunofluorescence confocal microscopy demonstrate the subcellular colocalization of SERCA2 with Bcl-2 and caveolin-1 in the ER of human fibroblasts. Importantly, SERCA2 does not colocalize with Bcl-2 associated with the mitochondria or with caveolin-1 associated with the plasma membrane.

DISCUSSION

There is a growing body of evidence that Ca^{2+} ions play a pivotal role in the regulation of cellular apoptosis. Regulation of apoptosis can occur at the level of the mitochondria and the ER. Proteins of the Bcl-2 family can modulate cellular calcium signaling, promote the leakage of Ca^{2+} from the ER, regulate the induction of apoptosis, and control the ER Ca^{2+} load. However, the exact underlying mechanisms are unclear, and conflicting reports about the effect of Bcl-2 on ER luminal calcium have been published.

Ca^{2+} is transported into the ER by SERCA and is released through either the IP_3R or the ryanodyne receptor. Along with various Ca^{2+}-binding proteins, SERCA and the IP_3R are responsible for the maintenance of the luminal Ca^{2+} concentration. Initially, a membrane pore forming activity of Bcl-2 was proposed as a potential mechanism of release of Ca^{2+} from the ER (*15*). However, this hypothesis was invalidated on grounds that the effect of Bcl-2 on Ca^{2+} signaling is independent of the pore-forming domain of the protein (*29*). An interaction of Bcl-2 with the IP_3R has been reported, specifically an effect of Bcl-2 on IP_3R phosphorylation (*20*, *30*). However, while Chen et al. (*20*) suggested that overexpression of Bcl-2 inhibited the IP_3R-induced release of Ca^{2+} from the ER lumen into the cytoplasm through inhibition of the IP_3R without changing the steady-state ER Ca^{2+} concentration, Oakes et al. (*30*) proposed that Bcl-2 activates Ca^{2+} release through the IP_3R. Part of this discrepancy may be caused by the use of different cell types and an effect of Bcl-2 overexpression on the levels of SERCA expression (*20*, *30*, *31*). The application of a genetically encoded sensor for Ca^{2+} imaging confirmed that Bcl-2-expressing cells suffer a decrease in ER Ca^{2+} concentration due to the Ca^{2+} leaking out of the ER (*21*).

The rate of Ca^{2+} leakage depends on SERCA expression (*7*, *21*). Overexpression of SERCA abolishes the inhibitory effect of Bcl-2 on apoptosis via modulation of Ca^{2+} homeostasis (*21*). Our data demonstrate a direct interaction of both Bcl-2 and Bcl-2Δ21 with SERCA1, resulting in a translocation of SERCA1 from CRD into a different membrane environment, and inactivation of SERCA. Others reported the co-IP of Bcl-2 also with the SERCA2b isoform (*31*). Bcl-2 inhibits SERCA1 in a manner independent of the presence of the C-terminal TM domain. However, the inhibition of SERCA1 is kinetically accelerated through the TM domain, which is apparent from a comparison of full-length Bcl-2 and Bcl-2Δ21. An important finding is the localization of SERCA to CRD in the SR. When either Bcl-2 or Bcl-2Δ21 is added to purified the SR, it is located, in part, to these CRD, and triggers a displacement of SERCA into a different membrane environment. It remains to be shown whether partial unfolding of SERCA, as detected through Cys labeling (*22*), is a prerequisite for or a result of this translocation. To date, the contact surfaces affording interaction between Bcl-2 and SERCA1 have not been established. Our results suggest that SERCA inactivation does not occur through a tight association of Bcl-2 with the ATP-binding domains or the high-affinity Ca^{2+}-binding domains of SERCA. However, it is possible that a transient interaction of Bcl-2 with these domains occurs, triggering a switch of SERCA into an inactive conformation, followed by the release of Bcl-2. In such a case, a change in either the apparent ATP or Ca^{2+} binding affinity of the remaining intact SERCA1 would not necessarily be observed.

Three major SERCA isoforms have been described. The SERCA2b and SERCA3 isoforms are widely expressed in different tissues, whereas SERCA1 and SERCA2a isoforms are specific and predominant isoforms in fast-twitch skeletal, slow-twitch skeletal, and heart muscle (*23*). All SERCA variants share sequence and functional homology; nevertheless, important features such as Ca^{2+} regulation of the Ca-ATPase activity vary significantly (*23*). Detailed structural investigations have provided insight into the conformational transitions of SERCA, which result in the transport of Ca^{2+} into the ER (*32*−*34*). An effect of sphingolipids, sterols, and lipids on SERCA activity has been demonstrated (*35*−*37*), suggesting that the structural and functional integrity of SERCA is sensitive to protein−lipid interactions. Hence, the location of SERCA within the CRD may control the activity of the enzyme. Several lines of evidence indicate that lipid microdomains such as CRD play an important role in the regulation of membrane-associated processes (*28*, *38*). CRD are generally enriched in cholesterol and/or sphingolipids. It is well-known that the ER is the site of sphingolipid and cholesterol synthesis, but their actual concentrations in the ER are low (*39*). Some authors suggest that the ER hosts membrane microdomains, though they are not clearly characterized (*40*−*43*). Moreover, a significant amount of caveolin is localized to the ER (*44*, *45*), consistent with the presence of CRD. In the study presented here, we demonstrate that SERCA1 is located to low-buoyant density fractions obtained by sucrose density gradient fractionation of SR, and colocalizes with caveolin-1 and caveolin-3, protein markers of CRD. This finding is greatly important as it suggests the regulation of SERCA activity through various protein−protein and lipid−protein interactions characteristic of CRD proteins. Caveolin-3 represents a muscle-specific isoform, whereas caveolin-1 detected in muscle usually originated from blood vessels, adipocytes, and satellite cells (*46*). Exogenous Bcl-2 or Bcl-2Δ21 added to the SR is distributed into the CRD fractions. These data suggest that the primary step in the inhibition of SERCA1 activity by Bcl-2 or Bcl-2Δ21 occurs in the CRD, followed by translocation of SERCA1. Incubation of SR with full-length Bcl-2 or Bcl-2Δ21 also displaces caveolin-1 and caveolin-3 from CRD, paralleled by the formation of caveolin-1 oligomers. This result indicates some coupling of translocation of SERCA and caveolin-1 from the CRD, suggesting that Bcl-2 modifies the microdomain membrane structure of the CRD. A direct interaction of Bcl-2 and SERCA1 was indicated through a binding assay, and SERCA1 was identified as a major SR protein that can bind to Bcl-2Δ21. However, this interaction is not stoichiometric, although an efficient inactivation of SERCA1 requires stoichiometric amounts of Bcl-2. Beyond the trivial possibility that the binding assay conditions may not reflect the actual conditions encountered in the SR in vivo and, thus, cannot be used for quantitation of protein−protein interactions, this finding may also suggest other possibilities: (i) a weak binding constant, (ii) indirect interaction between SERCA1 and Bcl-2 in the CRD of the SR, or (iii) a transient interaction followed by dissociation of the Bcl-2−SERCA1 complex as a result of SERCA1 destabilization and a conformational change (*22*).

The Bcl-2 family members share structural similarity with some bacterial toxins targeted to cell membranes (*14*, *15*, *17*). For instance, the B subunit of cholera toxin binds to GM1 gangliosides, and was used as a label for plasma membrane CRD (*43*). The similarity of the Bcl-2 structure with that of bacterial toxins, which have a demonstrated affinity for CRD, may indicate a general mechanism for the anti-apoptotic function of Bcl-2 based on the interaction of Bcl-2 with CRD lipids and proteins, altering the activity of CRD proteins.

Structural studies show that Bcl-2 is composed of eight α-helices with a hydrophobic groove on the surface (*14*). Bcl-2 and other anti-apoptotic Bcl-2 family members share sequence homology at the BH1−BH4 domains and the C-terminal hydrophobic domain. Mutational and structural analysis of the anti-apoptotic Bcl-2 family proteins revealed that the BH1 and BH2 domains are critical for heterodimerization with pro-apoptotic family members, thereby inhibiting their pro-apoptotic activity (*47*). The BH3 domains act as ligands during dimerization, and the BH1−BH3 domains form the hydrophobic groove into which the BH3 domain inserts (*48*). The BH4 domain appears to be responsible for the heterodimerization with other proteins regulating apoptosis (*49*−*51*). The TM domain targets the proteins to intracellular membranes, mostly of the mitochondria and ER (*52*, *53*). At present, we cannot specify which domains of Bcl-2 are responsible for the inhibition of SERCA activity; however, we can exclude the TM domain which contributes only to the kinetics of SERCA inhibition.

To date, co-immunoprecipitation experiments show an interaction of Bcl-2 with both SERCA1 (this paper and ref *22*) and SERCA2 (*31*). In normal human fibroblasts, we now demonstrate a partial colocalization of SERCA2 with Bcl-2 and with caveolin-1 in the perinuclear region consistent with ER localization. This partial colocalization likely reflects the physiological level of interaction between SERCA and Bcl-2 in vivo. Obviously, a total inactivation of SERCA is not desirable as such a condition can also trigger apoptosis, demonstrated in experiments with the specific SERCA inhibitor thapsigargin (*54*). However, physiological levels of Bcl-2 are much lower than those of SERCA, and our binding assay demonstrates a rather low affinity of Bcl-2 for SERCA. The Bcl-2−SERCA interaction may also be attenuated by complexation of Bcl-2 with other Bcl-2 family members and by sequence-specific phosphorylation of Bcl-2. To inhibit apoptosis, the interaction of Bcl-2 with SERCA simply has to lower the ER Ca^{2+} level below a threshold required to execute apoptosis.

REFERENCES

1. Hajnoczky, G., Davies, E., and Madesh, M. (2003) Calcium signaling and apoptosis, *Biochem. Biophys. Res. Commun. 30*, 445−454.
2. Green, D. R., and Reed, J. C. (1998) Mitochondria and apoptosis, *Science 281*, 1309−1312.
3. Zou, H., Li, Y., Liu, X., and Wang, X. (1999) An APAF-1/cytochrome *c* multimeric complex is a functional apoptosome that activates procaspase-9, *J. Biol. Chem. 274*, 11549−11556.
4. Thomenius, M. J., and Distelhorst, C. W. (2003) Bcl-2 on the endoplasmic reticulum: Protecting the mitochondria from a distance, *J. Cell Sci. 116*, 4493−4499.
5. Rizzuto, R., Pinton, P., Carrington, W., Fay, F. S., Fogarty, K. E., Lifshitz, L. M., Tuft, R. A., and Pozzan, T. (1998) Close contacts with the endoplasmic reticulum as determinants of mitochondrial Ca^{2+} responses, *Science 280*, 1763−1766.
6. Csordas, G., Thomas, A. P., and Hajnoczky, G. (1999) Quasi-synaptic calcium signal transmission between endoplasmic reticulum and mitochondria, *EMBO J. 18*, 96−108.
7. Scorrano, L., Oakes, S. A., Opferman, J. T., Cheng, E. H., Sorcinelli, M. D., Pozzan, T., and Korsmeyer, S. J. (2003) BAX and BAK regulation of endoplasmic reticulum Ca^{2+}: A control point for apoptosis, *Science 300*, 135−139.
8. Petersen, O. H. (2002) Calcium signal compartmentalization, *Biol. Res. 35*, 177−182.
9. Berridge, M. J., Bootman, M. D., and Roderick, H. L. (2003) Calcium signalling: Dynamics, homeostasis and remodelling, *Nat. Rev. Mol. Cell Biol. 4*, 517−529.
10. Demaurex, N., and Distelhorst, C. (2003) Cell biology. Apoptosis-the calcium connection, *Science 300*, 65−67.
11. Foyouzi-Youssefi, R., Arnaudeau, S., Borner, C., Kelley, W. L., Tschopp, J., Lew, D. P., Demaurex, N., and Krause, K. H. (2000) Bcl-2 decreases the free Ca^{2+} concentration within the endoplasmic reticulum, *Proc. Natl. Acad. Sci. U.S.A. 97*, 5723−5728.
12. Pinton, P., Ferrari, D., Magalhaes, P., Schulze-Osthoff, K., Di Virgilio, F., Pozzan, T., and Rizzuto, R. (2000) Reduced loading of intracellular Ca^{2+} stores and downregulation of capacitative Ca^{2+} influx in Bcl-2-overexpressing cells, *J. Cell Biol. 148*, 857−862.
13. Bassik, M. C., Scorrano, L., Oakes, S. A., Pozzan, T., and Korsmeyer, S. J. (2004) Phosphorylation of BCL-2 regulates ER Ca^{2+} homeostasis and apoptosis, *EMBO J. 23*, 1207−1216.
14. Petros, A. M., Olejniczak, E. T., and Fesik, S. W. (2004) Structural biology of the Bcl-2 family of proteins, *Biochim. Biophys. Acta 1644*, 83−94.
15. Schendel, S. L., Montal, M., and Reed, J. C. (1998) Bcl-2 family proteins as ion-channels, *Cell Death Differ. 5*, 372−380.
16. Sentman, C. L., Shutter, J. R., Hockenbery, D., Kanagawa, O., and Korsmeyer, S. J. (1991) Bcl-2 inhibits multiple forms of apoptosis but not negative selection in thymocytes, *Cell 67*, 879−888.
17. Strasser, A., Harris, A. W., Huang, D. C., Krammer, P. H., and Cory, S. (1995) Bcl-2 and Fas/APO-1 regulate distinct pathways to lymphocyte apoptosis, *EMBO J. 14*, 6136−61477.
18. Baffy, G., Miyashita, T., Williamson, J. R., and Reed, J. C. (1993) Apoptosis induced by withdrawal of interleukin-3 (IL-3) from an IL-3-dependent hematopoietic cell line is associated with repartitioning of intracellular calcium and is blocked by enforced Bcl-2 oncoprotein production, *J. Biol. Chem. 268*, 6511−6519.
19. Magnelli, L., Cinelli, M., Turchetti, A., and Chiarugi, V. P. (1994) Bcl-2 overexpression abolishes early calcium waving preceding apoptosis in NIH-3T3 murine fibroblasts, *Biochem. Biophys. Res. Commun. 20*, 84−90.
20. Chen, R., Valencia, I., Zhong, F., McColl, K. S., Roderick, H. L., Bootman, M. D., Berridge, M. J., Conway, S. J., Holme, A. B., Mignery, G. A., Velez, P., and Distelhorst, C. W. (2004) Bcl-2 functionally interacts with inositol 1,4,5-trisphosphate receptors to regulate calcium release from the ER in response to inositol 1,4,5-trisphosphate, *J. Cell Biol. 166*, 193−203.
21. Palmer, A. E., Jin, C., Reed, J. C., and Tsien, R. Y. (2004) Bcl-2-mediated alterations in endoplasmic reticulum Ca^{2+} analyzed with an improved genetically encoded fluorescent sensor, *Proc. Natl. Acad. Sci. U.S.A. 10*, 17404−17409.
22. Dremina, E. S., Sharov, V. S., Kumar, K., Zaidi, A., Michaelis, E. K., and Schöneich, C. (2004) Anti-apoptotic protein Bcl-2 interacts with and destabilizes the sarcoplasmic/endoplasmic reticulum Ca^{2+}-ATPase (SERCA), *Biochem. J. 383*, 361−370.
23. East, J. M. (2000) Sarco(endo)plasmic reticulum calcium pumps: Recent advances in our understanding of structure/function and biology, *Mol. Membr. Biol. 17*, 189−200.
24. Fernandez, L. J., Rosemblatt, M., and Hidalgo, C. (1980) Highly purified sarcoplasmic reticulum vesicles are devoid of Ca^{2+}-independent ('basal') ATPase activity, *Biochim. Biophys. Acta 599*, 522−568.
25. Lanzetta, P. A., Alvarez, L. J., Reinach, P. S., and Candia, O. A. (1979) An improved assay for nanomole amounts of inorganic phosphate, *Anal. Biochem. 100*, 95−97.
26. Kanski, J., Alterman, M. A., and Schöneich, C. (2003) Proteomic identification of age-dependent protein nitration in rat skeletal muscle, *Free Radical Biol. Med. 35*, 1229−1239.
27. Sharov, V. S., Galeva, N. A., Knyushko, T. V., Bigelow, D. J., Williams, T. D., and Schöneich, C. (2002) Two-dimensional separation of the membrane protein sarcoplasmic reticulum Ca-

ATPase for high-performance liquid chromatography−tandem mass spectrometry analysis of posttranslational protein modifications, *Anal. Biochem. 308*, 328−335.
28. Lucero, H. A., and Robbins, P. W. (2004) Lipid rafts: Protein association and the regulation of protein activity, *Arch. Biochem. Biophys. 426*, 208−224.
29. Chami, M., Prandini, A., Campanella, M., Pinton, P., Szabadkai, G., Reed, J. C., and Rizzuto, R. (2004) Bcl-2 and Bax exert opposing effects on Ca^{2+} signaling, which do not depend on their putative pore-forming region, *J. Biol. Chem. 279*, 54581−54589.
30. Oakes, S. A., Scorrano, L., Opferman, J. T., Bassik, M. C., Nishino, M., Pozzan, T., and Korsmeyer, S. J. (2005) Proapoptotic BAX and BAK regulate the type 1 inositol trisphosphate receptor and calcium leak from the endoplasmic reticulum, *Proc. Natl. Acad. Sci. U.S.A. 102*, 105−110.
31. Kuo, T. H., Kim, H. R., Zhu, L., Yu, Y., Lin, H. M., and Tsang, W. (1998) Modulation of endoplasmic reticulum calcium pump by Bcl-2, *Oncogene 17*, 1903−1910.
32. Toyoshima, C., Nakasako, M., Nomura, H., and Ogawa, H. (2000) Crystal structure of the calcium pump of sarcoplasmic reticulum at 2.6 Å resolution, *Nature 405*, 647−655.
33. MacLennan, D. H., Rice, W. J., and Green, N. M. (1997) The mechanism of Ca^{2+} transport by sarco(endo)plasmic reticulum Ca^{2+}-ATPases, *J. Biol. Chem. 272*, 28815−28818.
34. Andersen, J. P., and Vilsen, B. (1998) Structure−function relationships of the calcium binding sites of the sarcoplasmic reticulum Ca^{2+}-ATPase, *Acta Physiol. Scand. Suppl. 643*, 45−54.
35. Wang, Y., Tsui, Z., and Yang, F. (1999) Antagonistic effect of gangliosides GM1 and GM3 on the activity and conformation of sarcoplasmic reticulum Ca^{2+}-ATPase, *FEBS Lett. 457*, 144−148.
36. Lee, A. G. (1998) How lipids interact with an intrinsic membrane protein: The case of the calcium pump, *Biochim. Biophys. Acta 1376*, 381−390.
37. Starling, A. P., East, J. M., and Lee, A. G. (1993) Effects of phosphatidylcholine fatty acyl chain length on calcium binding and other functions of the (Ca^{2+}−Mg^{2+})-ATPase, *Biochemistry 32*, 1593−1600.
38. Fielding, C. J., and Fielding, P. E. (2003) Relationship between cholesterol trafficking and signaling in rafts and caveolae, *Biochim. Biophys. Acta 1610*, 219−228.
39. Lange, Y., Ye, J., Rigney, M., and Steck, T. L. (1999) Regulation of endoplasmic reticulum cholesterol by plasma membrane cholesterol, *J. Lipid Res. 40*, 2264−2270.
40. Sevlever, D., Pickett, S., Mann, K. J., Sambamurti, K., Medof, M. E., and Rosenberry, T. L. (1999) Glycosylphosphatidylinositol-anchor intermediates associate with Triton-insoluble membranes in subcellular compartments that include the endoplasmic reticulum, *Biochem. J. 343*, 627−635.
41. Gkantiragas, I., Brugger, B., Stuven, E., Kaloyanova, D., Li, X. Y., Lohr, K., Lottspeich, F., Wieland, F. T., and Helms, J. B. (2001) Sphingomyelin-enriched microdomains at the Golgi complex, *Mol. Biol. Cell 12*, 1819−1833.
42. Helms, J. B., and Zurzolo, C. (2004) Lipids as targeting signals: Lipid rafts and intracellular trafficking, *Traffic 5*, 247−254.
43. Fujinaga, Y., Wolf, A. A., Rodighiero, C., Wheeler, H., Tsai, B., Allen, L., Jobling, M. G., Rapoport, T., Holmes, R. K., and Lencer, W. I. (2003) Gangliosides that associate with lipid rafts mediate transport of cholera and related toxins from the plasma membrane to endoplasmic reticulm, *Mol. Biol. Cell 14*, 4783−4793.
44. Smart, E. J., Ying, Y. S., Mineo, C., and Anderson, R. G. (1995) A detergent-free method for purifying caveolae membrane from tissue culture cells, *Proc. Natl. Acad. Sci. U.S.A. 92*, 10104−10108.
45. Smart, E. J., Graf, G. A., McNiven, M. A., Sessa, W. C., Engelman, J. A., Scherer, P. E., Okamoto, T., and Lisanti, M. P. (1999) Caveolins, liquid-ordered domains, and signal transduction, *Mol. Cell. Biol. 11*, 7289−7304.
46. Hagiwara, Y., Nishina, Y., Yorifuji, H., and Kikuchi, T. (2002) Immunolocalization of caveolin-1 and caveolin-3 in monkey skeletal, cardiac and uterine smooth muscles, *Cell Struct. Funct. 27*, 375−382.
47. Yin, X. M., Oltvai, Z. N., and Korsmeyer, S. J. (1994) BH1 and BH2 domains of Bcl-2 are required for inhibition of apoptosis and heterodimerization with Bax, *Nature 369*, 321−323.
48. Sattler, M., Liang, H., Nettesheim, D., Meadows, R. P., Harlan, J. E., Eberstadt, M., Yoon, H. S., Shuker, S. B., Chang, B. S., Minn, A. J., Thompson, C. B., and Fesik, S. W. (1997) Structure of Bcl-xL-Bak peptide complex: Recognition between regulators of apoptosis, *Science 275*, 983−986.
49. Shibasaki, F., Kondo, E., Akagi, T., and McKeon, F. (1997) Suppression of signalling through transcription factor NF-AT by interactions between calcineurin and Bcl-2, *Nature 386*, 728−731.
50. Wang, H. G., Rapp, U. R., and Reed, J. C. (1996) Bcl-2 targets the protein kinase Raf-1 to mitochondria, *Cell 87*, 629−638.
51. Shimizu, S., Narita, M., and Tsujimoto, Y. (1999) Bcl-2 family proteins regulate the release of apoptogenic cytochrome *c* by the mitochondrial channel VDAC, *Nature 399*, 483−487.
52. Krajewski, S., Tanaka, S., Takayama, S., Schibler, M. J., Fenton, W., and Reed, J. C. (1993) Investigation of the subcellular distribution of the bcl-2 oncoprotein: Residence in the nuclear envelope, endoplasmic reticulum, and outer mitochondrial membranes, *Cancer Res. 53*, 4701−4714.
53. Akao, Y., Otsuki, Y., Kataoka, S., Ito, Y., and Tsujimoto, Y. (1994) Multiple subcellular localization of bcl-2: Detection in nuclear outer membrane, endoplasmic reticulum membrane, and mitochondrial membranes, *Cancer Res. 54*, 2468−2471.
54. Lam, M., Dubyak, G., Chen, L., Nunez, G., Miesfeld, R. L., and Distelhorst, C. W. (1994) Evidence that BCL-2 represses apoptosis by regulating endoplasmic reticulum-associated Ca^{2+} fluxes, *Proc. Natl. Acad. Sci. U.S.A. 91*, 6569−6573.

BI050800S